

## Processes of Defragmentation, Thermocapillary Extraction and Agglomeration of Ultradispersed Gold from Mineral Raw Materials and Technogenic Products within Laser Radiation Field

A.P. Kuzmenko<sup>1</sup>, I.V. Khrapov<sup>1</sup>, M.B. Dobromyslov<sup>2</sup>

<sup>1</sup> South-West State University, 94, 50 Let Otyabtya Str., Kursk, Russian Federation

<sup>2</sup> Pacific National University, 136, Tikhookeanskaya Str., Khabarovsk, Russian Federation

(Received 31 July 2013; revised manuscript received 11 October 2013; published online 17 October 2013)

According to the analysis of the results of complex studies of mineral raw materials and man-handle products containing ultra-dispersed gold, silver, and platinum before and after laser treatment, a qualitative physical model which explains the origin of thermal processes occurring under the action of laser radiation is proposed. It is noted that laser treatment of those materials generates processes of defragmentation, thermocapillary extraction, and agglomeration of micro- and nanoinclusions of these metals.

**Keywords:** Laser treatment, Defragmentation, Thermocapillary mechanism, Laser agglomeration.

PACS numbers: 61.80.Ba; 47.55.nb

### 1. INTRODUCTION

In extraction of valuable components especially of noble metals and platinoids (NMaPs) specific volume of power consumption on disintegration of the initial raw materials amounts to 70 % [1-3]. Moreover, the extraction of no nuggets inclusion is complicated by their both morphological and chemical structural features. Search for engineering solutions enhancing the efficiency of enrichment of NMaPs has widened to application of microwave frequency-, electro-pulse, magneto-pulse, electrochemical processing, electrodynamical and shock-wave impact, including their joint use on the initial mineral raw materials [4, 5]. In this connection, as shown earlier [6], laser processing concurrently secures defragmentation of hard native gold aggregates, thermocapillary extraction of ultra- and nanodispersive inclusions in NMaPs and their agglomeration in a melted state up to the formation of seen microstructures the size down to several hundredths of micrometers after which their further extraction may be implemented in a gravitational way. Data in existence on laser processing of such materials can really be of practical value. This paper analyses the physical process initiated by laser radiation (LR), namely, defragmentation, thermocapillary extraction, and agglomeration.

### 2. EXPERIMENTAL RESULTS AND DISCUSSION

In analyzing data from the processing of these materials it was taken into consideration that the critical role when LR impacts heterogeneous and heterophase media (HPM) (the materials belong to these media) is played by thermal processes due to optical absorption according to Bouguer-Lambert-Beer's law:  $I(z) = I_0(1 - R)\exp(-\alpha z)$ . In all these experiments the LR intensity did not surpass the limit of the linear area, i.e.  $I_0 < I_{cr}$ , was fulfilled, where  $I_{cr}$  is the value of the LR intensity starting from which the nonlinear effects appear. Despite this, in this region as well the absorption coefficient applied to the system under investigation is of a complex nature. In this case, as shown in many papers, analysis can be ex-

cuted by numerical methods only [7], and for simple assessed calculations as the absorption coefficient its averaged magnitude  $\alpha = (\alpha_1 + \alpha_2 + \dots + \alpha_n)/n$  can be taken. Here  $\alpha_1, \alpha_2, \dots, \alpha_n$  are reference data.

It is obvious that in more general analysis one must take into account dispersion dependence:  $\alpha^* = (\alpha_1^* + \alpha_2^* + \dots + \alpha_n^*)/n$ . Here  $\alpha_1^*, \alpha_2^*, \dots, \alpha_n^*$  are complex absorption coefficients of each component that make up natural and technogenic structures. In this case every component of the absorption coefficient- has real ( $\alpha'_i$ ) and imaginary ( $\alpha''_i$ ) components:  $\alpha_i^* = \alpha'_i + i\alpha''_i$  ( $i = (-1)^{1/2}$  is imaginary unit). For further consideration one should take into account the fact that the LR monochromaticity simplifies the situation considerably. In doing so, the cross over to the analysis relative to the averaged magnitude –  $\alpha$  becomes well-grounded.

So, in analyzing the processes one can determine the energy whose value is responsible for the primary effects such as heating, defragmentation, melting, evaporation, combustion, thermal oxidation, ionization, and plasma formation with consecutive crystallization and transition into condensed state. The magnitude of this energy also governs secondary effects such as optical breakdown, deformation, and radiation absorption by plasma.

Of note is the fact that normalized in mass contribution of every physical parameter such as the absorption coefficient  $\alpha$  and also all other physic-chemical ones is proposed to be considered. Such parameters, for instance, are specific heat -  $c$ , melting heat -  $\lambda$ , evaporation heat -  $L$ , coefficients of thermal diffusivity -  $\chi$  and heat transfer -  $\eta$ , and other characteristics of processes that occur in laser processing. To determine the contribution of every mineral that constitutes the given compound under investigation the use of, for instance, data of X-ray phase analysis and reference data were allowed. For inhomogeneous in composition and structure powder materials the magnitude of  $\chi$  is low and varies within  $10^{-6} - 10^{-7}$  m<sup>2</sup>/s, which corroborates the equilibration of processes that take place. For comparison, its value in metal materials is several magnitudes greater (Cu =  $1.12 \times 10^{-4}$ , Ag =  $1.65 \times 10^{-4}$  m<sup>2</sup>/s) and is sharply reduced for oxides of these metals. Thus, under

our circumstances, only equilibrium heat processes should occur. The diagram that graphically shows thermal processes in LR processing with the intensity  $I_0$  is given in Fig. 1, where also shown is a powder material formed as a regular cylinder. In terms of this, let's write the end heat balance equation in averaged physical parameters  $c$ ,  $\lambda$ ,  $L$  and  $\eta$ :

$$Q_{LR} = cm\Delta T + \lambda m_{mel.} + Lm_{ev.} + \eta\pi d(T_{mel.} - T_{min.mel.}), \quad (1)$$

where  $m$  is the total mass of HPM,  $m_{mel.}$  and  $m_{ev.}$  are masses of evaporated and melted HPM, respectively,  $d$  is the focus spot diameter,  $T_{mel.} = (T_{1mel.} + T_{2mel.} + \dots + T_{nmel.}) / n$  is the averaged melt temperature, and  $T_{min.mel.} = \min\{T_{mel.}\}$  is the minimum melt temperature characteristic of HPM.

In the right-hand side of equation (1) one must take into consideration the effect of thermochemical reactions, namely the portion of chemically-reacted substance in HPM that follows the Arrhenius law  $\partial N / \partial t = Kf(N)\exp(-E_a / kT)$ . Here  $N$  is the concentration of chemically-reacted substance;  $K$  is the coefficient that determines the reaction rate and incorporates collision frequency of reacting particles;  $f(N)$  is the function corresponding to the reaction mechanism;  $E_a$  is the activation energy;  $k$  is the Boltzmann constant.

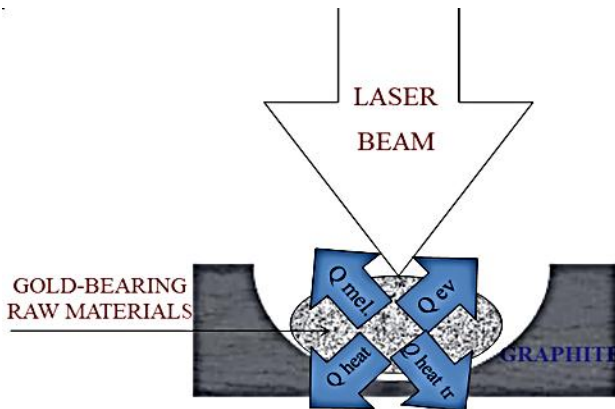


Fig. 1 – Redistribution of the incident laser beam energy

The relation between the incident radiation energy  $E$  and the activation energy satisfies the condition  $E_a - E > 0$ . In doing so, this condition is fulfilled virtually for all compounds. The magnitude  $f(N) = 1$  will correspond to the maximum reaction yield of interaction between LR and HPM, which secures the maximum yield of the desired reagent  $N = N(T_{max})$ . Such result can be achieved at  $T = T_{max} \sim T_{ил.}$ . From this one can evaluate the upper limit of the reaction time  $t_p$  obtained from the Arrhenius law:  $t_p = N(T_{max}) \times \exp(-E_a / kT) / K$ . For instance, the predicted time of the reduction reaction for common natural mineral compounds  $SiO_2$  or  $CaSiO_3$  [8] will be equal to  $t_p = 1200$  and  $5000$  s, respectfully. The consideration of this contribution would be significantly complicated (1), which is seen from equation [9], which can be written in the following way:  $\partial(\delta T) / \partial t + T(\rho c v)(\partial p / \partial T)_p \nabla v = (Q_v + \rho N q_{ch.react.}) / \rho c v$ . Here  $p$  is pressure and  $T$  is the medium temperature, on which the density  $\rho = \rho(p, T)$  depends.  $\delta p, \delta p, \delta T$  are variations of  $p, T$  due to the me-

dium heating by LR and the heat released during chemical reaction.  $c v$  is the specific heat at constant volume;  $Q_v$  is the heat released at radiation absorption in volume unit;  $q_{ch.react.}$  is the amount of heat released by the mass unit in chemical reactions;  $v$  is the speed of thermal front motion, which coincides with the particle velocities in melt. The solution to this equation is hardly possible. The assessment of the low limit for the time of HPM processing by laser radiation turns out to be less than a minute, making it practically meaningful.

The spot of the defocused LR has a diameter  $d = 4 - 6$  mm and its velocity is  $v$ . It is supposed that for the system under investigation (multiphase powder) the distance of heat transfer is comparable with the diameter. The heat transfer takes place over the distance not greater than three spot's diameters. It should be noted that this presumption is well-grounded because the heat transfer coefficient  $\eta$  for such complex systems is critically low. For instance, if for gold its value is  $320 \text{ W}/(\text{m} \times \text{K})$ , then oxide shapes of other components is characterized by the magnitude of several units.

A consideration of the size of heat transfer area that coincides with the direction of LR travel makes it possible to find the time in which the heat transfer is critical  $t = 3d / v \sim 10 - 20$  s. In this case at the stationary mode of laser processing it is possible to cross to the heat transfer equation in the integral form useful for calculations  $Q_{heat tr.} = \eta\pi d(T_{mel.} - T_{min.mel.})$ . Such a choice of the low limit for the heat transfer temperature stems from the fact that the melted mass of one of the components begins to crystallize as it cools, which is accompanied by the release of  $Q_{cr.}$ . In this case, the heat transfer sign is changed and  $Q_{mel.}$  will be released inversely.

With consideration for the above comments concerning the equality in module of heats needed for melting and released in crystallization they should have been cancelled. However, firstly, we are predominantly interested in melting; secondly, it should be kept in mind that the LR source moves. Therefore, the heat release as a result of crystallization takes place behind the melt front and it is unlikely to play role in every succeeding point of processing. Moreover, the amount of heat released is relatively small  $Q_{cr.} = -\lambda m$ . The estimation reveals that the mass of crystallizing substance determined in approximation of melt hemisphere with radius  $R = d / 2$ :  $m = 2/3(\rho\pi R^3)$  and magnitude  $\lambda$  taken with consideration of averaged provides the value of energy crystallization much less than  $Q_{cr.} \ll Q_{LR}$ , making it possible to consider only the energy of the LR source in the right-hand side of (1).

As noted above, the processing mode secures the minimum evaporation, therefore  $m_{ev.} \ll m$ , making it possible to ignore this contribution to the right-hand side of heat balance equation. The energy loss of the incident LR must include also  $Q_{pl.fl.}$ , the energy absorbed by the plasma flame,  $Q_r$  the energy reflected from the surface,  $Q_{g.ej.}$  the energy carried away by the gas ejection.

Let's discuss their role. The intensity of applied LR was significantly lower than threshold values starting from which the electron avalanche and multiple photon ionization ( $10^{11} \text{ W}/\text{cm}^2$ ) and even the evaporation gas breakdown ( $10^8 - 10^9 \text{ W}/\text{cm}^2$ ) take place. This fact made it possible to ignore these losses. Only powder PHM

were processed by LR that have high dispersion up to the wavelength of applied LR  $\lambda = 1.06 \mu\text{m}$ , with the result that the reflection was vanishingly small  $Q_r$ . The magnitude  $Q_{g.ej}$  can also be ignored since the processing mode was chosen in such a way that either to exclude or significantly reduce its portion. It should be noted as well that heat outflow into the substrate made as a cylindrical cell was not considered either, since it was specially made from reactor high dispersive graphite whose thermal conductivity is reduced with increasing temperature (at room temperature  $-170$ , and at  $1700^\circ\text{K} - 51 \text{ W} / (\text{m} \times \text{K})$ ) up to  $T_{\text{mel.}} = 2200^\circ\text{K}$ . The reflection coefficient from the cell walls at applied LR wavelength  $1060 \text{ nm}$  is also minimum, making it possible to ignore the component. All of this justifies the validity of heat balance equation in the form (1).

The detailed analysis of processes initiated by LR on PHM was made earlier [10, 11], where the following processes were noted as major:

- defragmentation (disintegration);
- extraction of ultra- and nanodispersive gold;
- agglomeration.

Despite seeming continuity of these processes they are changes of rather differing level. At first stage with the help of thermal concentrated and speedy effect of LR it is possible to find aggregates with inclusions of ultra- and nanodispersive NMaPs no nuggets inclusion. At the second stage the hydrodynamic extraction mechanism occurs  $\frac{\partial}{\partial t} \delta p + \rho \nabla \vec{V} = 0$ , and the motion of

particles survived in the melt is described by the hydrodynamic equation:  $\frac{\partial}{\partial t} \delta \vec{V} + \frac{\nabla \delta p}{\rho} = 0$ . Here and further

the velocity of particle motion is introduced, which is generally coincides with the melt front travel velocity  $v = v_{\text{mel.}}$ . At the final stage, when the material underwent transition into a liquid phase state, the surface tension dominates, which is corroborated by the formation from the melt structures of spherical shape.

To carry out more profound analysis let's write (1) in the following way:

$$I_0 A = K v_{\text{mel.}} \rho (L_{\text{ev.}} + L_{\text{mel.}} + c(T_{\text{mel.}} - T_{\text{min.mel.}})). \quad (2)$$

Included in (2) is  $I_0$  – density of power (intensity) of LR, and  $A$  is its absorption coefficient. For estimate calculations it is adopted in (2) that  $K$  is a dimension coefficient at which  $K \times v_{\text{mel.}} = V$  is the melt volume. The volume of melted PHM mass per minute is obviously dependent on the processing velocity of LR (laser beam translation). Obviously, the practical processing mode of PHM is such at which the beam translation velocity will coincide with the ravel velocity of the melt wave. The estimate calculations that consider the PHM composition and mass fraction of individual averaged physical magnitudes provide important for practice values of a stationary travel velocity of the melt wave deep into the products under processing ( $v_{\text{mel.}}$ ) and the melt time of the filling layer ( $t$ ). So, the estimation of  $v_{\text{mel.}}$  gives

$$v_{\text{mel.}} = I_0 A / \rho (L_{\text{mel.}} + C(T_{\text{mel.}} - T_{\text{min.mel.}})) \sim 300 \text{ m/s} \quad (3)$$

which is lower than the averaged sound speed in pro-

cessed products, and this signifies that non-stationary processes in melting products of processing are ruled out since  $v_{\text{mel.}} \ll v_s \sim 2 \times 10^3 \text{ m/c}$ . With consideration for  $\chi$  – thermal diffusivity averaged for every components of the material and  $l_{\text{mel.}}$  the second important parameter of processing, namely, the melt time of filling layer can be determined:

$$t = \chi \pi (\rho l_{\text{m.z.}} C (T_{\text{mel.}} - T_{\text{min.mel.}}) / (2 I_0 L_{\text{mel.}}))^2 \sim 10^{-8} \div 10^{-6} \text{ s} \quad (4)$$

This renders pulsed laser processing (with durations of up to hundredths of microseconds) practical and economically sound.

High travel velocity of the melt wave front in PHM under study (3) that have a wide scatter of values for  $T_{\text{mel.}}$  and  $L$  does not exclude the existence of evaporation in laser processing of low-melt compounds. Therefore, in addition to defragmentation gas-jet mechanism for the destruction of the initial compounds becomes possible, which was shown in electron microscopical study (Fig. 2) of the surface of gold thin film (thickness not greater than  $1 \mu\text{m}$ ) that appears during laser processing. At the surface output channels of gas jets with diameter within  $1 \mu\text{m}$  are clearly seen.

To explain the extraction processes of dispersed and ultradispersed gold that accompany laser processing it must be considered that the internal energy of the compounds is dictated by both the surface tension energy of the systems under study and the LR intensity (from  $60$  to  $450 \text{ W/cm}^2$ ) at which they undergo transition to a liquid phase state.

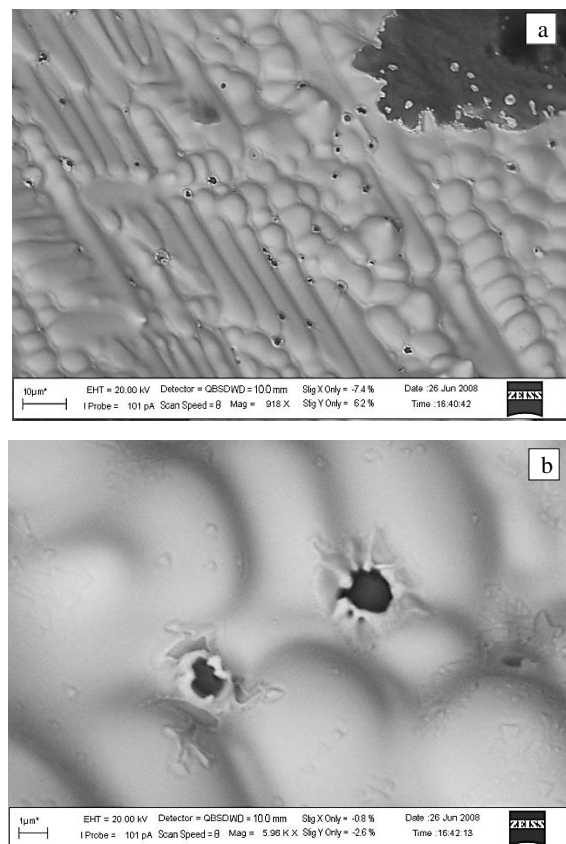
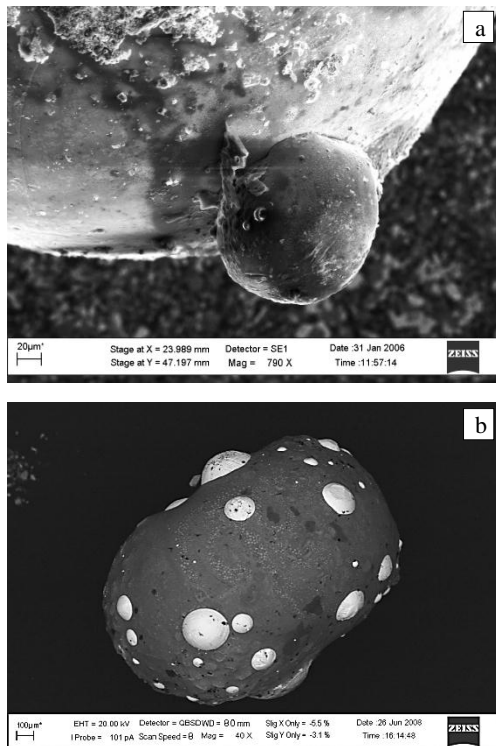


Fig. 2 – Scan electron-microscopic pattern of the thin gold foil surface with marks of gas jet break

Discuss the role of surface tension in observed phenomena. In a liquid state PHM under study must follow the additive principle (the Antonov law):  $\sigma_{12} = \sigma_1 - \sigma_2$ , where  $\sigma_{12}$ ,  $\sigma_1$ ,  $\sigma_2$  are surface tension of individual phases and their compounds. Consider wetting angles between the liquid gold and other part of melted mass using their electron-microscopic patterns shown in Fig. 3. Surface tension of liquid phase heavy concentrate  $\sigma_1$  (Fig. 3a) was only slightly lower than  $\sigma_2$  for the melt of agglomerated gold. In this case only partial wetting occurred since the wetting angle was slightly lower than  $\pi/2$  as is seen in Fig. 3a.



**Fig. 3** – Scan electron pattern of structure for clay (a) and heavy concentrate (b) of a gold-bearing sample after laser processing

As accompanying phase alumino-silicates make themselves evident widely due to their natural occurrence in gold-bearing systems, as this was the case for most compounds studied including those given further.

## REFERENCES

1. R.M. Hough, R.R.P. Noble, M. Reich, *Ore Geol. Rev.* **42**, 55 (2011).
2. N.M. Chrnyhov, V.V. Abramov, V.S. Kuznetsov, *Vestnik VGU. Series: Geology* **2**, 110 (2009).
3. V.A. Chanturia, *Gorn. Magazine* **12**, 64 (2005).
4. H. Ernest, *Can. Mineral.* **40**, 419 (2002).
5. A. Cabral Rafael, B. Lehmann, R. Kwitko, P.D. Jones, *Miner. Mag.* **65**, 169 (2001).
6. N.A. Leonenko, A.P. Kuzmenko, I.V. Silyutin, I.Yu. Rasskazov, G.V. Sekisov, M.A. Gurman, G.G. Kapustina, N.L. Shvets, *Patent RF N2413779*, 07.10. 2010, C22B11/02, B2.
7. E.V. Kharanzhevsky, S.N. Kostenkov, *Vestnik Udmurtskogo Univers. Physics. Chemistry* **5**, 33 (2012).
8. V.P. Zhdanov, *The chemical reaction rate* (Novosibirsk: Nauka: 1986) [In Russian].
9. N.V. Karlov, N.A. Kirichenko, B.S. Kukynchuk, *Laser Thermochemistry* (Moscow: Nauka: 1992).
10. A.P. Kuz'menko, I.Yu. Rasskazov, N.A. Leonenko, G.G. Kapustina, I.V. Silyutin, J. Li, N.A. Kuz'menko, I.V. Khrapov, *J. Min. Sci.* **47**, 850 (2011).
11. N.A. Leonenko, V.I. Kharchenko, N.A. Kuzmenko, I.V. Silyutin, I.V. Khrapov, A.P. Kuzmenko, *Tech. Phys. Lett.* **35**, 837 (2009).

Their surface tension turns out to be significantly lower than that of NMaPs. So for laser sinters of high-clayey sands with inclusions of ultra- and nanodispersed gold (Fig. 3b) the wetting angle found to be dramatically greater than  $\pi/2$ . This follows also from comparing  $\sigma_1$  and  $\sigma_2$ :  $\sigma_1 \ll \sigma_2$ . Comparison of wetting angles for heavy concentrate and high-clayey sands provides nearly two-fold difference, which correlates with difference of  $\sigma_1$  and  $\sigma_2$  for them. It should be noted that virtually for all the systems studied clear-cut interfaces between the products of the laser remelt occurred.

The gold foil thickness in Fig. 2 that forms in agglomeration of ultra- and nanodispersed gold is not greater than several microns. By using this parameter according to [12] let's establish the extraction mechanism making choice between two potential mechanisms, namely, thermocapillary and thermal gravitational-capillary mechanisms. It is characteristic that both are proportional to the surface tension gradient ( $\partial\sigma/\partial x$ ). Dominant role of one or another mechanism can be established from the estimate of the value for the Bond figure, which equals the ratio of figures of Marangoni's and Raleigh's and is easily reduced to  $K_{Bond} = \rho g \chi h^4 / \sigma$ . Here  $g$  is the acceleration of gravity;  $\chi$  is temperature conductivity;  $h$  is the layer thickness;  $\sigma$  is the medium surface tension. The estimate of the Bond figure with consideration for known values of  $\rho$ ,  $g$ ,  $\chi$ ,  $\sigma$  and observed experimentally on the foil thickness (not greater than several micrometers) turns out to be dramatically lower than unity. Thus, one can conclude that in laser agglomeration of ultra- and nanodispersed gold (may be other NMaPs as well) just thermal capillary mechanism contributes the most.

## 3. CONCLUSION

Thus, in laser processing there is always sequence of the above processes, namely, defragmentation (disintegration), extraction of ultra- and nanodispersed gold, and laser agglomeration. Agglomeration, the so called coalescence, makes it self-evident as the end result of the action of surface tension gradient when the motion of dispersed and ultradispersed gold particles to the surface of melt is accompanied by their uniform agglomeration up to the formation of visible thin foil, as is shown in Figs. 2 and 3.